

# Towards computerized typology and classification of ceramics

Ayelet Gilboa<sup>a</sup>, Avshalom Karasik<sup>b,c\*</sup>, Ilan Sharon<sup>c</sup>, Uzy Smilansky<sup>b</sup>

<sup>a</sup> The Zinman Institute of Archaeology, University of Haifa, Mount Carmel, Haifa 31905, Israel

<sup>b</sup> Department of Physics of Complex Systems, The Weizmann Institute of Science, Rehovot 76100, Israel

<sup>c</sup> Institute of Archaeology, The Hebrew University, Jerusalem 91904, Israel

Received 28 July 2003; received in revised form 26 October 2003; accepted 29 October 2003

## Abstract

We report on newly developed mathematical and computational tools for morphological description, classification and analysis of archaeological artifacts. The need for such tools is most acutely felt, due to two main factors: (1) The lack of objective, quantitative criteria for shape analysis, classification and *comparanda*; (2) The overwhelming abundance of data, which renders impossible any extensive comparative typological analysis using traditional methods. We shall describe the main ideas which distinguish our method, and demonstrate its applicability by presenting the analysis of two assemblages of Iron Age ceramics from sites in Israel.

© 2003 Elsevier Ltd. All rights reserved.

**Keywords:** Pottery; Typology and classification; Ceramic profiles; Curvature analysis; Near Eastern Iron Age archaeology; Phoenician pottery

## 1. Introduction

Artifacts are by definition the direct products of human action. As such, they convey significant information regarding various cognitive and behavioral aspects of both their producers and users. Archaeologists who study assemblages of such artifacts seek to identify in them distinctive patterns that can be used for drawing inferences regarding a plethora of issues, from straightforward spatial and temporal settings, to higher-range issues such as technological and cognitive capabilities, motor skills, symbolic assertions and negotiations, social, ethnic and other identities, economic activities, and more.

There are two basic techniques by which archaeological research approaches artifacts analysis:

1. *Typological classification*, where the numerous artifacts are clustered into discrete ‘types’, and the assemblage is sorted according to these pre-defined types. Underlying this approach is the assumption that artifacts were produced according to, and there-

fore can be classified into, discrete templates. Such classification raises serious issues—what is a ‘type’? Is there an objective way of classifying artifacts to ‘types’? (For a pioneering concern with these questions, see for example [22]) Is the choice of types optimal (keeping the number of types to a minimum, while losing minimal information).

2. An alternative approach is *attribute analysis*, in which artifacts are described according to a set of selected attributes, and which seeks to establish a direct correlation between one (or arrays) of these attributes and temporal sequences, spatial associations, or cultural patterns. The main problem of this approach is how, among the myriad of attributes usually observed in a large assemblage of artifacts, can one isolate a subset which varies intelligibly with the facets under study.

In practice, most archaeologists bring both of these approaches to bear, depending on the problem at hand.

In both approaches, *shape* attributes are among the most fundamental properties by which artifacts are characterized and studied. These include the description of the general shape of the artifact, defined by its *contour* (the line which marks its boundary or cross section), as

\* Corresponding author. Tel.: +972-8-93-44-987; fax: +972-8-93-44-109

E-mail address: fekarasi@wisemail.weizmann.ac.il (A. Karasik).

well as the description of particular shape properties, considered to be significant for specific archaeological issues. Traditional shape descriptions and classifications, however, rely on intuitive, often vague characterizations, which are hard to quantify. Terms such as ‘everted/inverted rim’, ‘squat body’, ‘high carination’, or even ‘elegant curves’, which do not have a unique interpretation, are commonly used. Early attempts to base the analysis solely on measurable attributes have been constrained to using a poor vocabulary of simple metrics (length, width, radius, etc.) or combinations thereof (see [38,46]). Most of the shape information is lost when using such extremely reductionist statistics, and the meaningful comparison of assemblages based on them may be problematic.

More recent studies aimed at quantitative analysis of ceramic attributes describe the profiles as mathematical curves. One of the earliest methods is the ‘tangent-profile’ (TP) or its later development the ‘sampled tangent-profile’ (STP) technique [31]. The curve is described by providing the tangent as a function of the arc-length. (This is related to the method used here, since the curvature is the first derivative of the tangent angle.) A related method was used by Liming et al. [36], who expressed the shape by providing the distance of the points on the profile from the axis of revolution as a function of the arc-length. Gero and Mazzullo [13] used Fourier series to describe archaeological artifacts, but their method can hardly be applied to the analysis of ceramic sherds. Hagstrum and Hildebrand [19] introduced the ‘two-curvature’ method by which vessels are described by the curvature along two axes. They use this method to get an overall view of assemblages, such as e.g., the percentages of common shapes (open or closed) and to obtain approximate volumes. They did not use their tools for classification, typology or intensive comparison of vessels shapes.

The GOAD project (Graphically Oriented Archaeological Database) concentrated on the development of archaeological database, which enables a user-friendly search. To compare shapes they used the Generalized Hough Transform (GHT) [10,33]. Several other techniques, which make use of the profiles of the vessels as curves, are summarized in the book of Orton et al. [39, pp. 152–165]. A good summary of ‘line geometry’ with some applications to surfaces of revolution, such as archaeological vessels can be found in Pottmans et al. [41].

The use of powerful mathematical and computational methods in archaeological attribute analysis is steadily growing. Sablatnig and Menard [43], Adler et al. [1] and Razdan et al. [42] use digitized information as a convenient access for extracting quantitative measures for various features of the profile, such as the location of corners or inflection points, rims and necks (see also websites [23–25]). Kalvin et al. [29], Leitão and Stolfi [32]

and Leymarie et al. [34] concentrate on illustrating excavated archaeological sites using virtual reality (websites [26–28]). The last two also deal with the problem of ‘virtual mending’ of vessels, using the fragments outlines’ curvature to match neighboring sherds. Again, they hardly apply their methods for typological analysis.

In typical excavations on *tells* in the Near East, pottery is found in huge quantities. The intuitive, manual clustering of thousands of artifacts (often, as in large stratigraphical excavations—millions) is a Sisyphean labor at best, and the process of finding culturally meaningful parallels for them among millions of illustrations in published excavation reports is rapidly becoming impossible. The traditional ‘hunt for parallels’ is currently carried out by spending months in specialized research libraries, checking out scores of excavation reports and leafing through thousands of pages, containing uncountable illustrations. Still, the placing of a given pottery assemblage in its proper spatial and temporal setting is, and always will be, a mandatory process, without which higher-level meanings of the assemblage cannot be assessed. Reliable publications/studies of large artifactual assemblages are becoming rare, and severely delay, often for decades, the publication of site reports.

Moreover, due to the limitations imposed by the traditional means of publication, only a fraction of the excavated material appears in the reports of any but the smallest excavations. The selection of the items to appear in print introduces a bias. The standard procedure, especially in medium to large excavations, has been to illustrate what the analyst considers a ‘type’—and supplement this with quantitative data regarding the distribution of the various types (usually—per temporal phase). Selection may be unavoidable, but its outcome is that the reader may not be able to assess the defined ‘types’, as these are illustrated by very few examples, often just one. Sometimes the very fact that quantitative data have been provided is perceived as legitimizing a reduction in the number of (costly) illustrations. Thus the quantitative data provided is difficult to evaluate: how must one relate to a statement asserting that ‘Stratum X had 500 examples of Type Y’ if one has no clear idea of the variability *within* type ‘Y’? Worse—what if, in one’s own typology, type ‘Y’ is equivalent to either type ‘A’ or ‘B’ or partly type ‘C’ (the other part of ‘C’ being type ‘Z’ in the *comparanda*)?

Thus, one of the major problems faced by archaeologists is to find optimal methods by which assemblages can be presented, described and analyzed. Such a method should be concise, yet as comprehensive as possible, so as to encompass as much information as possible about the studied objects. It should avoid the subjectivity of traditional typologies. It must take advantage of modern means for database construction, to

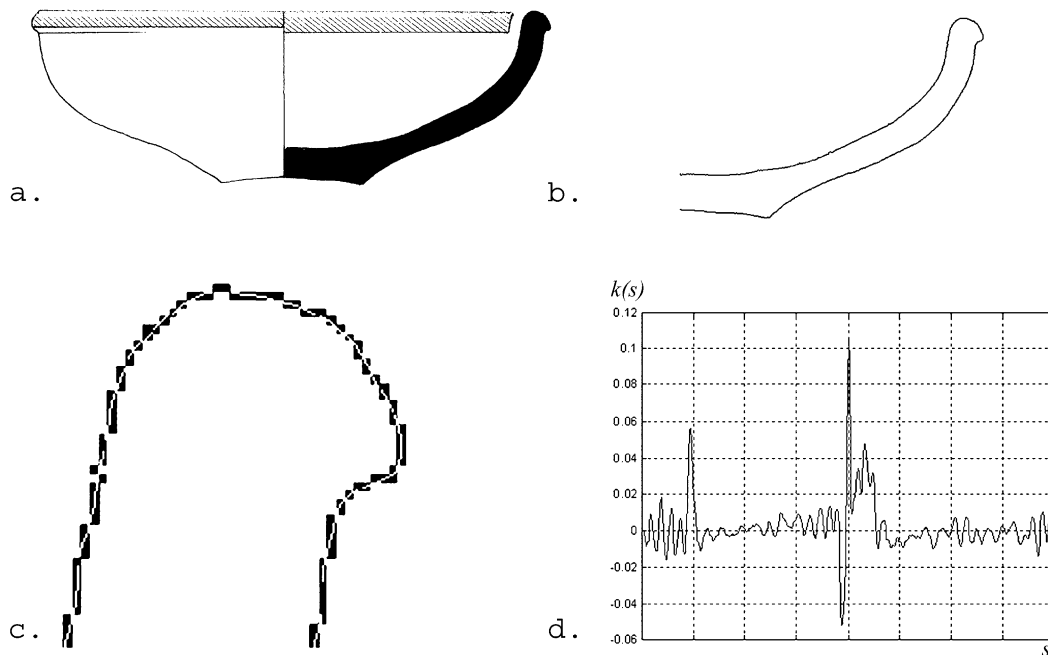


Fig. 1. The steps leading from a scanned drawing to the curvature function. a. A scanned drawing of a bowl. b. The pixelized profile. c. Enlarged detail of the pixelized profile and the interpolated curve. d. The curvature function.

enable exhaustive storage and systematic search and retrieval algorithms. Considering the aspects mentioned above, computer-aided artifact analysis is naturally called for.

The work presented here pertains to typology and classification which are confined to shape attributes. Extensions of the technique to include additional attributes (size, decorations, ware, composition) are self-evident, but for the purpose of this exposition we chose to concentrate on shape (of cross-sections) alone.

The input consists of drawings of pottery in printed archaeological reports, and the analysis is based on the contour defined by the drawn cross-sections. We are well aware of the problems inherent in using manual drawings as the basis for subsequent analysis [39, pp. 89–93; 40]. However, the records of past (and most present) excavations are only accessible in this form, and thus analyses based on such media are, and in the foreseeable future will be, unavoidable.

As will become clearer below, we do not restrict the cross sections to present *whole vessels*, nor do we assume that the cross sections are simply connected (in other words, handles can form a part of the analyzed shape). On the other hand, the system is constrained to pieces containing at least a fragment of the rim. We use the tip of the rim as the point of origin for comparisons and the rim radius for size-standardization. As pointed out above, most Near-Eastern and Mediterranean excavations suffer more from over-abundance of sherds than from dearth. Thus reducing the sample to rims only, and deleting body-sherds which are often only minimally

informative, is not too high a price. Restricting it to complete profiles only may well lead to sample-size problems, as well as to over-representation of restricted spatial locations or temporal episodes where complete vessels happened to be better preserved.

We should emphasize that our aim at this point is limited to providing the archaeological research with descriptive and analytical tools. The interpretation of these results, and their evaluation within the archaeological/cultural context is definitely beyond our scope here, though in the examples presented below the interpretive potential is readily evident.

We shall proceed according to the following order: the next section is of a more mathematical nature. It presents our method for the analysis of ceramic cross-sections as planar curves. The section which follows is dedicated to shape analysis and typological study of two archaeological assemblages. These preliminary studies demonstrate the potential stored in this line of work. The concluding section is a summary presenting various sources of inherent limitations and uncertainties, alongside further directions which are now being investigated.

## 2. Computerized typological analysis of ceramic profiles and cross sections

### 2.1. Data acquisition

The first step in the analysis transforms the contours to be analyzed in digital form. This is done by scanning

linear drawings, prevalent in archaeological reports and transforming them to a standard form. Figure 1a–d illustrates the sequence of operations. A typical drawing from an archaeological report (Fig. 1a) is scanned, and a boundary identification procedure yields a pixelized version of the contour (Fig. 1b). In this form, it contains irrelevant ‘noise’, which is due to the finite resolution of the scanning device, imperfections of the original drawings, etc. These features are filtered out to yield the smooth, yet accurate presentation of the original boundary (Fig. 1c).

Technically, the smoothing is implemented by first Fourier transforming the vectors of the  $x$  and  $y$  coordinates along the curve. The irrelevant high-frequency fluctuations are attenuated by a convenient filter function:

$$f(l) = \frac{1}{1 + \exp[(l - l_0)/d]} \quad (1)$$

where  $l$  is the Fourier index,  $l_0$  is the filtering threshold and  $d$  gives the width of the transition domain. Transforming back to real space, we get the smooth coordinate functions which are the basis of the subsequent analysis.

## 2.2. The curvature function

Our analysis is based on the description of a planar curve in terms of its *curvature function* [35,37]. The curvature at each point on the curve is defined by constructing the circle, which osculates the curve at the point of interest. The curvature is the inverse of the circle’s radius, and it is positive if the curve is convex at that point and negative if it is concave (Fig. 1d). The position of a point on the curve is specified by the distance  $s$  along the curve (from an arbitrary reference point). The curvature function  $\kappa(s)$  provides the curvature as a function of the arc length  $s$ .

An alternative definition of the curvature can be obtained by considering the vector  $\mathbf{t}(s)$  which is the tangent to the curve at points.  $\theta(s)$  denotes the direction of the tangent. The curvature  $\kappa(s)$  is defined as the rate of change of  $\theta(s)$  at  $s$ :

$$\kappa(s) = \frac{d\theta(s)}{ds} \quad (2)$$

Clearly, the curvature vanishes for straight lines, and is largest at sharp angles.

Given the curvature function  $\kappa(s)$ , the curve is completely specified. This can be easily shown by integrating  $\kappa(s)$  once to obtain  $\theta(s)$ , from which another integration provides the coordinates of the curve. Gauss’ theorem states that for a *closed* curve:

$$\oint \kappa(s) ds = 2\pi. \quad (3)$$

This follows immediately by integrating (2) along the closed curve. This identity is valid independently of the shape of the curve (provided that it is connected and not self intersecting), and it is important for controlling errors, which may arise in the numerical analysis.

We chose to represent the curves in terms of their curvature function because this method has several intrinsic advantages:

- **Relevance**—the curvature is most sensitive to the distinctive features, which are most often used for morphological typologies, such as rims, carination points, etc.
- **Uniqueness**—the original curve and its curvature function are in one-to-one relation. Each can uniquely and accurately be reconstructed from the other.
- **Efficiency**—a single function of one variable, describes a two-dimensional line.
- **Invariance**—the curvature function does not change under translations and rotations of the frame of reference.

The extraction of the curvature function from numerical data poses a few problems which are discussed in the literature (see [11,30]). The main problem stems from the fact that the curvature involves the second derivative of the contour, and numerical differentiation introduces large errors. However, the computation of the derivatives in Fourier space corresponds to a multiplication, which introduced no extra error, and the high frequencies are not sufficiently amplified to overcome the exponential filtering which was used. We checked this numerical scheme by comparing the original profile with the one reconstructed from the numerically computed curvature. The root mean square (RMS) deviation between the two is of an order of magnitude less than  $10^{-4}$  of the total length of the curve.

Features, which are significant for morphological description, classification and analysis, are expressed now in terms of the curvature function. Thus, the degree of similarity between artifacts can be quantified by measuring the ‘distance’ between curvature functions. Mathematically, there is a considerable spectrum of legitimate measures of this ‘distance’ and this is where the archaeological preference is injected into the analysis. This freedom allows attributing different weights to different kinds of features (e.g., emphasizing the rim more than the shoulder in the analysis of pottery). Here, the dialogue between archaeology and mathematics is crucial. Note that choosing one’s distance function and / or differentially weighting it to reflect what one judges to be archaeologically significant features for the question at hand in no way jeopardizes the objectivity of the method as long as one consistently uses the same function and parameters across the relevant sampling space.

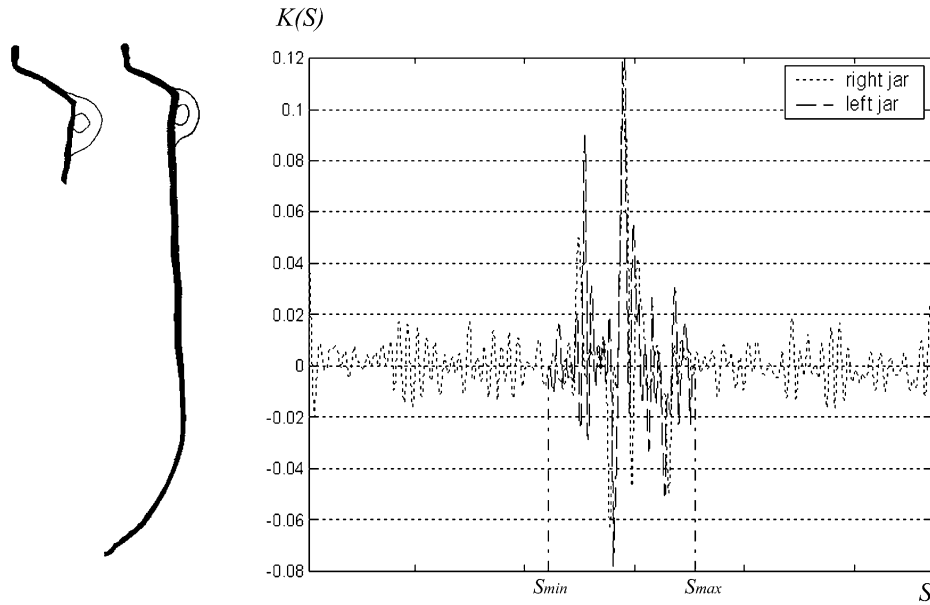


Fig. 2. The profiles of two unequal sherds (left) and their curvature functions (right) centered at the common rim point.

### 2.3. Comparing profiles by comparing their curvature functions

As noted above, the method we propose is designed to treat rim-sherds as well as complete profiles. The former present an added complication in that we have to compare cross-sections which do not necessarily present the same fractions of the original whole vessels. Once we allow for that, whole vessels (or complete profiles) can be included as special cases which do not need special treatment.

Two important assumptions have to be made in order to proceed with the analysis: that the cross-section represents a surface of revolution and that the drawn section is properly positioned relative to the axis of revolution. If these assumptions hold, the highest point of the profile corresponds to the rim of the vessel. Its distance from the axis of revolution is the rim radius, which is the only length scale we can determine unambiguously from a drawing of a potsherd. We use the highest point as a reference point from which distances along the curve are measured, and we use the rim radius as the unit of length. Thus, the highest point occurs at  $s=0$  where the tangent to the contour is perpendicular to the symmetry axis, with  $\theta(0)=\pi$ . The scaling of arc length by the radius is very important, because it enables the comparison of vessels which are similar in all their attributes, but for their absolute size. Moreover, in this way, the curvatures of all the sherds to be analyzed are scaled, and their rim points appear at the same value of  $s$ , namely at  $s=0$ . The end points of the smallest fragment in the assemblage, to be denoted by  $s_{\min}$  and  $s_{\max}$ , set the limits of the common  $s$  interval over

which the comparison between curvature functions will be performed. Two unequal jars with their scaled and centered curvature functions are illustrated in (Fig. 2).

In order to compare two fragments (denoted by  $\alpha$  and  $\beta$ ) we have to define the ‘distance’  $d_{\alpha\beta}$  between the corresponding curvature functions  $\kappa_{\alpha}(s)$  and  $\kappa_{\beta}(s)$  in the  $s$  interval  $[s_{\min}, s_{\max}]$ :

$$d_{\alpha\beta} = \sqrt{\int_{s_{\min}}^{s_{\max}} (\kappa_{\alpha}(s) - \kappa_{\beta}(s))^2 \omega(s) ds} \quad (4)$$

In the definition above, we introduced the *weight function*  $\omega(s)$  which is assumed to be non-negative in the interval  $[s_{\min}, s_{\max}]$ . This function allows the archaeologist to introduce her/his judgment concerning the relative importance of the various features in the compared fragments. For example, if the entire contour is of the same relevance for the comparison, one would take  $\omega(s)=1$ . Another example: If the part of the contour, which belongs to the interior, is of less archaeological relevance, a lower value of the weight function can be assigned to this part of the interval. To remove some features altogether,  $\omega(s)$  is set to zero in the corresponding domains.

The *scalar product* of two curvature functions is defined with a similar weight:

$$\langle \alpha | \beta \rangle = \int_{s_{\min}}^{s_{\max}} \kappa_{\alpha}(s) \kappa_{\beta}(s) \omega(s) ds. \quad (5)$$



The *correlation* between two curvatures functions is:

$$C_{a,\beta} = \frac{\langle a|\beta \rangle}{\sqrt{\langle a|a \rangle \langle \beta|\beta \rangle}}. \quad (6)$$

The distance between two curvature functions and their correlation are intimately connected, as can be seen from the identity:

$$(d_{a\beta})^2 = \langle a|a \rangle + \langle \beta|\beta \rangle - 2\sqrt{\langle a|a \rangle \langle \beta|\beta \rangle} C_{a,\beta} \quad (7)$$

Clearly,  $C_{a,\beta}=1$  if and only if the two curvature functions are identical, and the distance between them is zero. This is the maximum value of the correlation. The smaller  $C_{a,\beta}$  is, the less similar the compared functions are.

A possible weakness in the system proposed above is over-dependence on the axis origin ( $s=0$ ). The highest point on the profile may not have been accurately determined, especially when the shred is small, and/or the rim is fairly flat. **This is overcome by maximizing the correlation between any two curves with respect to a small shift in the position of their maxima.**

#### 2.4. Prototype generation and shape interpolation

The implicit assumption behind typological analysis is that artifacts with similar attributes can be reduced to a single ‘ideal’ or ‘mean’ specimen, which represents the entire group. We shall refer to this representative sample as ‘prototype’. Most often, a prototype is defined by selecting a few samples that manifest in the best way the attributes which distinguish the type. After defining the prototypes, each relevant specimen in the assemblage is to be assigned to the prototype to which it bears maximal affinity.

The representation of the profiles in terms of their curvatures is particularly convenient for the generation of a prototype. Let  $\kappa_a(s)$  with  $a=1\dots N_A$  be the curvatures of  $N_A$  sherds which define the type A. The mean curvature function,

$$\kappa_A(s) = \frac{1}{N_A} \sum_{a=1}^{N_A} \kappa_a(s) \quad (8)$$

provides the curvature of a *virtual* profile which picks up the attributes which are common to the samples in the defining set. (In the sequel, we shall use capital subscripts to denote prototypes.) Suppose that another prototype is similarly represented by a mean curvature  $\kappa_B(s)$ . The distance  $d_{A,B}$  between the two prototypes should be sufficiently large to allow a meaningful sorting. (Formally, we must require that  $d_{a,A} \ll d_{A,B}$  and  $d_{\beta,B} \ll d_{A,B}$  for all the samples in the sets which define the prototypes.) If this condition is fulfilled, we can sort the

potsherds with respect to the distance from the prototypes, or equivalently define their correlations with the prototypes.

Assume that a given assemblage, which consists of  $M$  profiles (with curvature functions  $\kappa_m(s)$ ,  $m=1, \dots, M$ ) are to be sorted according to their affinity to  $D$  predetermined prototypes  $\kappa_{A_1}(s), \kappa_{A_2}(s), \dots, \kappa_{A_D}(s)$ . Going over all the assemblage, we find for each profile, say the  $\kappa_m(s)$ , the ‘coordinates’  $x_1(m), x_2(m), \dots, x_D(m)$  such that:

$$\kappa_m(s) = \sum_{i=1}^D x_i(m) \cdot \kappa_{A_i}(s) + \lambda_m(s) \quad (9)$$

The last term in (9) is necessary since the prototypes do not span the entire space of curvature functions.  $\lambda_m(s)$  stands for that component of  $\kappa_m(s)$  which is *orthogonal* to the subspace spanned by the prototypes. To obtain the coordinates  $x_i(m)$  we take the scalar product of  $\kappa_m(s)$  with each of the prototype curvatures. Since, by definition,  $\lambda_m(s)$  is orthogonal to these functions, we obtain a set of  $D$  linear equations which is solved by inverting the symmetric matrix  $\hat{A} = \langle A_i | A_j \rangle$ .

$$\begin{bmatrix} \langle A_1 | A_1 \rangle & \langle A_1 | A_2 \rangle & \langle A_1 | A_3 \rangle & \cdots & \langle A_1 | A_D \rangle \\ \langle A_2 | A_1 \rangle & \langle A_2 | A_2 \rangle & \langle A_2 | A_3 \rangle & \cdots & \langle A_2 | A_D \rangle \\ \langle A_3 | A_1 \rangle & \langle A_3 | A_2 \rangle & \langle A_3 | A_3 \rangle & \cdots & \langle A_3 | A_D \rangle \\ \vdots & \vdots & \vdots & \ddots & \vdots \\ \langle A_D | A_1 \rangle & \langle A_D | A_2 \rangle & \cdots & \cdots & \langle A_D | A_D \rangle \end{bmatrix} \begin{bmatrix} x_1(m) \\ x_2(m) \\ x_3(m) \\ \vdots \\ x_D(m) \end{bmatrix} = \begin{bmatrix} \langle A_1 | m \rangle \\ \langle A_2 | m \rangle \\ \langle A_3 | m \rangle \\ \vdots \\ \langle A_D | m \rangle \end{bmatrix} \quad (10)$$

(A solution of the equation exists only if  $\det \hat{A} \neq 0$ , that is, if the prototypes are linearly independent. This can be tested in practice by ensuring that

$$\frac{D^D}{D!} \cdot \frac{|\det \hat{A}|}{\sqrt{\left( \prod_{i=1}^D \left[ \sum_{j=1}^D \langle A_i | A_j \rangle^2 \right] \right)}}$$

is not too different from 1.) Each profile is now represented by a point  $\mathbf{x}(m)$  in a  $D$ -dimensional space. Once the coordinate vectors  $\mathbf{x}(m)$  are known, we can easily compute the *magnitude* of the vectors  $\lambda_m(s)$  which we denote by  $|\lambda_m(s)|$ . The assumption that the assemblage can be sorted by the prototypes  $\kappa_{A_1}, \kappa_{A_2}, \dots, \kappa_{A_D}$  is justified only if the ‘quality factors’

$$\zeta_m \equiv \frac{\|\lambda_m\|^2}{\langle m | m \rangle} = 1 - \sum_{i=1}^D x_i(m) \frac{\langle m | A_i \rangle}{\langle m | m \rangle} \quad (11)$$

are small. Clearly,  $\zeta_m$  vanishes if  $\kappa_m(s)$  is indeed in the space spanned by the prototypes, and it equals one (which is its maximal value) if  $\kappa_m(s)$  is orthogonal to all the prototypes.

The general formalism presented above takes a simple and transparent form when only two prototypes are used ( $D=2$ ).

$$\begin{aligned} x_1 &= \frac{\langle m|A_1\rangle\langle A_2|A_2\rangle - \langle m|A_2\rangle\langle A_2|A_1\rangle}{\langle A_1|A_1\rangle\langle A_2|A_2\rangle - \langle A_2|A_1\rangle^2} \\ x_2 &= \frac{\langle m|A_2\rangle\langle A_1|A_1\rangle - \langle m|A_1\rangle\langle A_1|A_2\rangle}{\langle A_1|A_1\rangle\langle A_2|A_2\rangle - \langle A_2|A_1\rangle^2} \end{aligned} \quad (12)$$

Note that when  $\kappa_m(s)$  equals  $\kappa_{A_1}(s)$ ,  $(x_1, x_2) = (1, 0)$  and if it equals  $\kappa_{A_2}(s)$ ,  $(x_1, x_2) = (0, 1)$ . We shall make use of (12) in the analysis to be reported in the next section.

After assigning to each fragment in the assemblage its coordinates  $x_1(m), x_2(m), \dots, x_D(m)$  and the quality factors  $\zeta_m$ , we can study the typology in greater detail. The underlying assumption, that the predetermined  $D$  prototypes can indeed characterize the assemblage, is tested by the values of the quality factors. If large values ( $\zeta_m > 0.5$ ) appear consistently, the corresponding fragments have features which are essentially orthogonal to all the prototypes, in other words—the set of prototype is insufficient. Assuming that the quality factors are small, one can test the distribution of the points which correspond to the fragments, in the  $D$ -dimensional space. If the choice of prototypes represents a true partition of the assemblage, the points should concentrate predominantly in the vicinity of the pure prototypes. However, clustering of points can occur also at other values, showing that the assemblage prefers types which are intermediate between the original prototypes. This can happen, e.g., when the assemblage covers a few periods during which one could distinguish a gradual typological variation. This possibility will be discussed below, and will be illustrated in the next section.

A frequent assumption is that ‘types’ gradually change over time, space, or some other variable of archaeological interest. In such cases, it is convenient to demonstrate the transition between the types along a linear axis. For this purpose, we can generate an interpolating sequence of (again *virtual*) profiles, which interpolate between the two prototypes:

$$\kappa_\mu(s) = \mu\kappa_{A_1}(s) + (1-\mu)\kappa_{A_2}(s) \text{ for any } 0 \leq \mu \leq 1. \quad (13)$$

We can also compute for each profile in the assemblage the value of the interpolating parameter  $\mu(m)$  once its coordinates  $(x_1(m), x_2(m))$  have been extracted. Special care must be taken when this parameter is derived, since in contrast with the interpolation sequence (13), typical profiles in the assemblage possess a non-vanishing  $\lambda_m$  component (see equation (9)), which is orthogonal to the prototypes. The expression we use for the interpolating parameter is

$$\mu(m) = \frac{x_2(m)}{x_1(m) + x_2(m)} \quad (14)$$

which, in most cases, takes values in the range (0,1) and assumes the extreme values when the profile is equal to one of the prototypes. Finally we should comment that much of the present analysis would have taken a simpler form, if the prototype curvature functions were an orthonormal set. Since this is not the case, the treatment presented above is called for.

In the following two sections we shall show how the concepts defined above are used to our advantage in typological analysis of assemblages from Iron Age sites in the Southern Levant: Dor, Hazor and Tyre.

### 3. Applications of computerized shape analyses

The present section reports on two examples where the methods discussed above are applied to archaeological problems of current interest. The data-base for the analysis consisted of drawings of vessels (or potsherds), and in each of the cases we had at our disposal approximately eighty items. Thus, we could not aim at high statistical significance. Our purpose was mainly to check the ability of the computerized analysis to emulate the skill and intuition of the ceramics experts, and to check whether we can possibly surpass them.

#### 3.1. Shape development in early Iron Age bowls from Tel Dor

The early Iron Age ceramic sequence at Dor has important bearing on issues of early Iron Age chronology and cultural interaction throughout the Mediterranean [17,18,45]. The temporal evolution of bowls was considered one of the most instrumental chronological indexes for the early Iron there. Clearly, a heavy burden of proof rests on minute changes in exact rim shape and a precise and objective method for describing and comparing such stylistic developments is called for.

The assemblage consists of 86 bowls excavated from stratified loci which are attributed to temporal horizons termed (from early to late) late Ir1a, Ir1a|b, Ir1b, Ir1|2 and Ir2a. These horizons follow each other in a rapid temporal sequence. These bowls were analyzed by Gilboa [15,17], and an evolution of (mainly) rim shape was identified. The samples shown in Fig. 3 represent the change in the rim shape, from the ‘complex’ (C)—typical of the late Ir1a horizon, to the ‘simple’ (S)—typical of the Ir1b, Ir1|2 and Ir2a horizons, via a transitional type (T), typifying the Ir1a|b. Employing visual judgment only, the three types were defined as follows: The complex (C) type: carinated bowls with short upper walls and thick molded rims with inner and outer

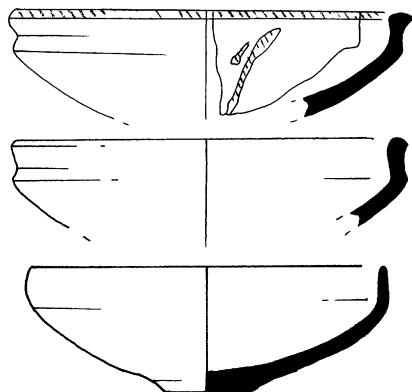


Fig. 3. The transition from complex (top) to transitional (middle) to simple (bottom) rim shapes.

projections, the inner one usually more thick and rounded. The transitional (T) type: carinated bowls with molded rims, but generally smaller and thinner, the walls above carination point shorter and the rim closer to the carination point and much less accentuated; the inner projection of the rim has nearly disappeared. The simple (S) type: carinated bowls with short, usually vertical upper walls and hardly any rim treatment. However, it was recognized, that for each ‘type’, recurrent ‘subtypes’ could be defined. Also, it was obvious that the bowl repertoire (understandably) did not transform completely from one horizon to the next, and that in each horizon, some ‘earlier’ types were in evidence. Whether this is due to the fact that bowls from different ‘types’ were indeed being produced concurrently, or alternatively—some ‘earlier’ specimens remained in circulation, or that their presence in later assemblages is due to various site formation processes (e.g., re-deposition)—cannot be established.

Using a few samples which represent the C and the S types, we generated the mean profiles for the (virtual) respective prototypes. The samples used to define the C prototype, and the shape of the resulting prototype are shown in (Fig. 4). The virtual forms which interpolate between the two extremes (see equation (13)) are shown in (Fig. 5), where  $\mu$  changes between 0 and 1 in steps of  $\Delta\mu = 1/9$ . One of the aims of the analysis described below was to determine whether the ‘transitional’ type represents an independent prototype, or that the data are consistent with an evolution as described in (Fig. 5). This will be the case if profiles (points) cluster away from the S and C prototypes in the C–S plane, without apparent deterioration of the ‘quality factors’  $\zeta$ .

We used two methods to display the results of the analysis. In the first, we attributed to each vessel in the assemblage two coordinates with respect to the C and the S prototypes, respectively, using equation (12). The results are shown in (Fig. 6a–e), where each point corresponds to a fragment in the assemblage, and the

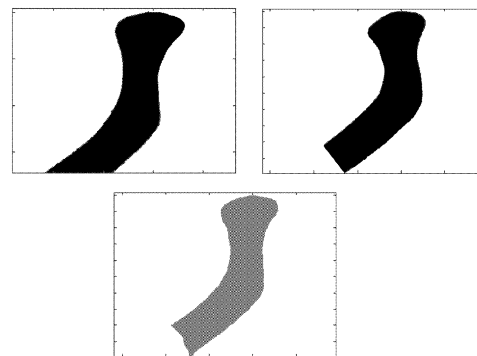


Fig. 4. Two profiles, which represent the complex type and the corresponding (virtual) prototype (bottom).

symbols used for the points represent their stratigraphical identity. The distribution of the points in the C–S plane clearly supports the original claim that the shape of the rim evolves from the C to the S type during the studied period. The same data is summarized in (Fig. 6f), which shows the distribution of the interpolating parameters  $\mu$  that increase over time (see equation (14)). Again, the potsherds from different horizons are analyzed separately, and the typological evolution is apparent in the shift of the distributions from the along the C–S axis.

Together with the computation of the coordinates and the extrapolation parameters, we computed the ‘quality factors’  $\zeta_m$  defined in equation (11). For each period its mean value is less than 0.25 which supports the use of two prototypes in the analysis. The (T) type alluded to above, can be accounted for by interpolation. The ‘virtual’ linear interpolation with  $\mu \approx 0.55$  produces a profile which is almost identical to the empirically derived ‘T’ prototype, with  $\zeta_T \approx 0.15$ . This is an example of a situation in which a type defined as a cluster in the space of shapes, can be accounted for by interpolation between two extreme prototypes.

### 3.2. Morphological typology of late Iron Age commercial jars from Hazor and Tyre

An important issue in archaeological research is the identification and interpretation of commercial links between different regions and polities (e.g., [9,12,44]). To this end one must determine the origin of the vessels uncovered in excavations. Physical and chemical tests (petrography, neutron activation analysis etc.) can offer a partial answer, but their high cost usually limits their use en masse. Typological analysis is thus commonly employed to augment, direct or even replace those tests. In the context of the Iron Age Levant, the identification of commercial links between Phoenicians and Israelites has been a focus of some interest, especially vis-à-vis the allusions to such contacts in the bible.



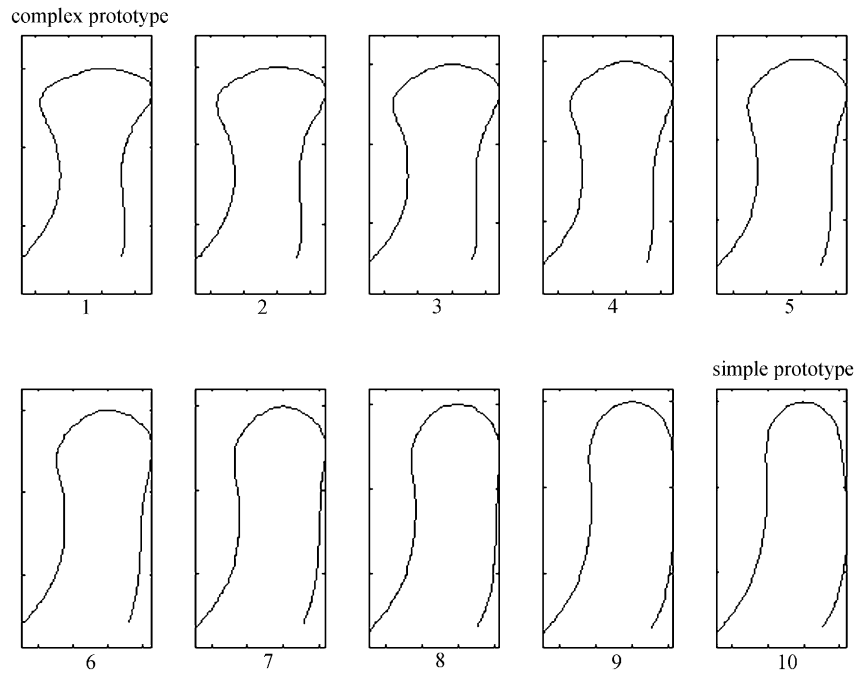


Fig. 5. Interpolating forms from 'complex' (upper left) to 'simple' (lower right).

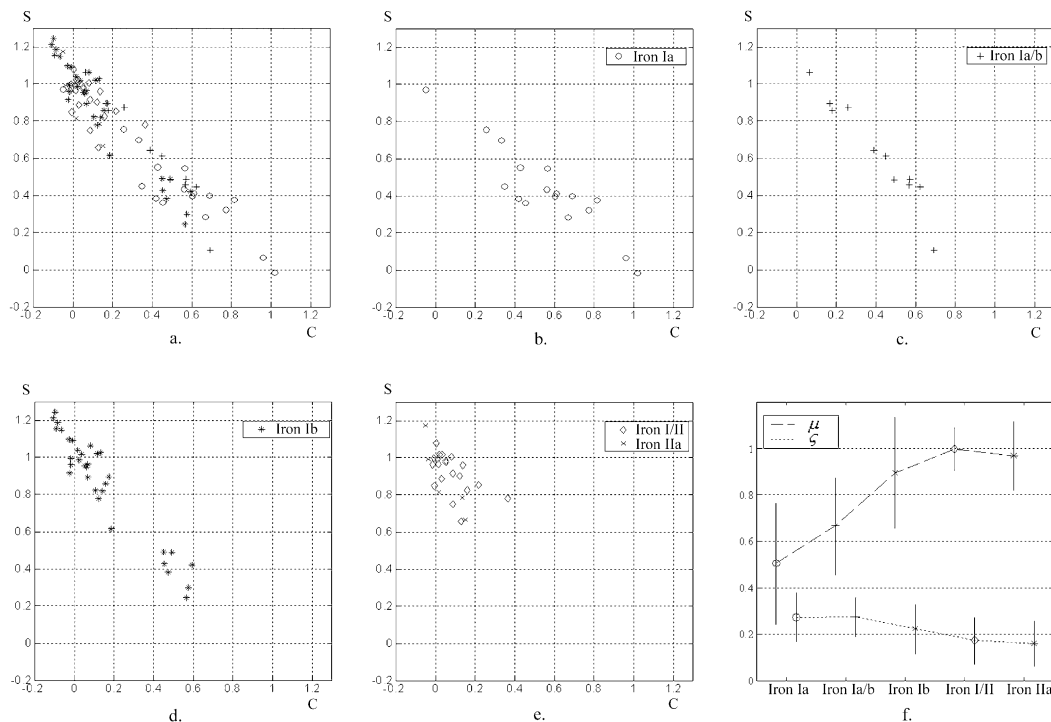


Fig. 6. a. The distribution of the bowls in the C-S plane, denoted by the same stratigraphic symbols as used in b–e. b–e. The same as a. for either one or two horizons. f. The mean values and the standard deviations of  $\mu$  and  $\zeta$  for each period.

Ninth and eighth century BCE cylindrical (so called 'torpedo' or 'crisp-ware') commercial jars became first known from sites in Israel, especially its northern part, in regions known to have formed part of the

northern Israelite Kingdom during the Iron Age IIB. The largest assemblage uncovered was that at Hazor, in the Huleh basin in Israel's north. In the 1970s similar jars were uncovered in an excavation conducted

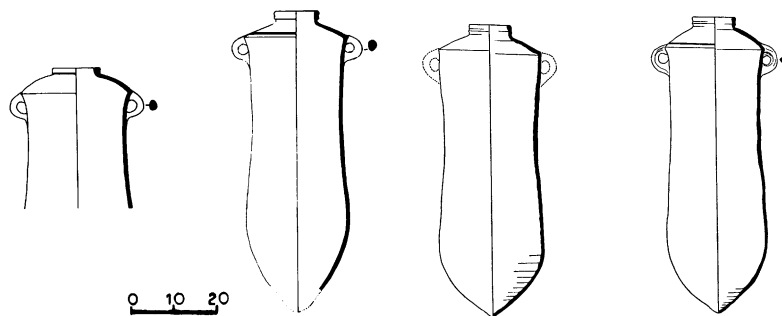


Fig. 7. Four 'torpedo' storage jars from Hazor (the two to the right; [48, pl. 72: 8–9]) and from Tyre (the two to the left; [6, pl. 4: 4–5])

at Tyre, one of the major Phoenician centers in Lebanon (Fig. 7).

One scholar [14] concluded that these jars were produced in the Kingdom of Israel—and thence were exported to Tyre (for the reasons underlying her choice of Israel as the place of production and not vice versa, see *ibid.*). In contrast, Tyre's excavator [5] reached the opposite conclusion—that the jars found at Tyre were manufactured at Tyre and if anything—the occurrence of similar ones at Hazor points to an export in the opposite direction. These disagreements notwithstanding, the Hazor=Tyre jars are cited in major textbooks as one of the clearest attestations of trade links between Israel and Phoenicia (e.g. [4, p. 48]). A third study, however [16, p. 11] denied the possibility of reconstructing trade relations between the two sites based on these jars, claiming that subtle morphological differences (especially rim shapes) between the jars uncovered at Tyre and those at Hazor prove that they form two discrete groups. (The importance of differentiating between rim-shapes of these commercial jars has also been recognized by Anderson [2, pp. 197–199, types SJ-15–SJ-17].)

To test our computerized method, we scanned and computed the curvature for all the 'torpedo' jars published in the respective excavation reports (for Tyre: [6, pls. 2: 1–10; 3: 1–8; 4: 1–6]; for Hazor: [48, pls. 72: 1–4, 6–9; 73: 2, 4–6, 8, 10, 12–16; 90: 1–4; 91: 1–7, 9–12, 14, 15; 101: 9–15]; [47, pls. 180: 20; 229: 11–13]). We computed the *correlations matrix* for the combined assemblage (which consists of 24 vessels from Tyre and 47 from Hazor). A *cluster analysis* of the correlation matrix reveals the inner structures of the assemblages. The correlation tree (Fig. 8) consists of vertices (which stand for real or virtual profiles) connected by branches, which indicate affinities and hierarchical order. The provenance of a profile is indicated by the symbol drawn at the vertex: \* for Tyre profiles, ° for Hazor profiles, and just a dot for virtual profiles. The tree is generated recursively. In the first step, the  $M \times M$  correlation matrix is computed ( $M=71$  in the present case), and the pair with the highest correlation, say  $(i,j)$ , is identified. Two vertices are drawn at the height  $y=C_{ij}$  and the

symbols that indicate their provenances are used. The horizontal distance between the points is arbitrarily fixed to a value  $\Delta x$ , and the pair is positioned at the middle of the  $x$  interval. The mean profile  $\kappa_{(i,j)} = \frac{1}{2}(\kappa_i + \kappa_j)$  is computed, and added to the list of profiles, while the two original profiles are eliminated. This ends the first step, where now the effective assemblage consists of only  $M-1$  profiles. At the next step, the  $(M-1) \times (M-1)$  correlation matrix is computed, and the pair with the highest correlation, say  $(k,l)$ , is identified. If  $k$  and  $l$  stand for real profiles, the procedure described previously is repeated, and the pair of vertices is drawn at a horizontal position  $x'$  which is not occupied already by a higher pair in the tree. If one of the profiles is virtual, it is drawn at the height  $y=C_{k,l}$ , and its horizontal position is the midpoint between its 'parents' position. Finally, the vertex (which is now just a point) is connected to the 'parents' vertices by branches. The other member of the pair is drawn a distance  $\Delta x$  away, and the corresponding symbol is used. Again, the 'parent' pair is replaced by their average, and the number of effective profiles is reduced by 1. This procedure is repeated until the assemblage is exhausted when it consists of 2 profiles.

The cluster analysis is summarized in a correlation tree (Fig. 8), where distinct branches indicate well-segregated morphological types. The parameter  $\Delta x$  may be increased as  $M$  decreases, and the strict rules of drawing can be relaxed for the sake of visual clarity. As can be seen in (Fig. 8), more than 90% of the jars from Tyre are on one branch, and about 80% of the jars from Hazor are on the other. This provides a visual indication that the degree of mixing in the combined assemblage is significantly lower than random. However, the fact that the two branches meet at a correlation level of 0.7–0.8 indicates that the mixed assemblage indeed consists of rather similar jars, and the clustering is sensitive to quite refined details.

To sharpen the test, we defined two prototypes, selected to represent the mean features of 'pure' subsets of the jars uncovered at Hazor and Tyre respectively. We computed the coordinates of every jar in the

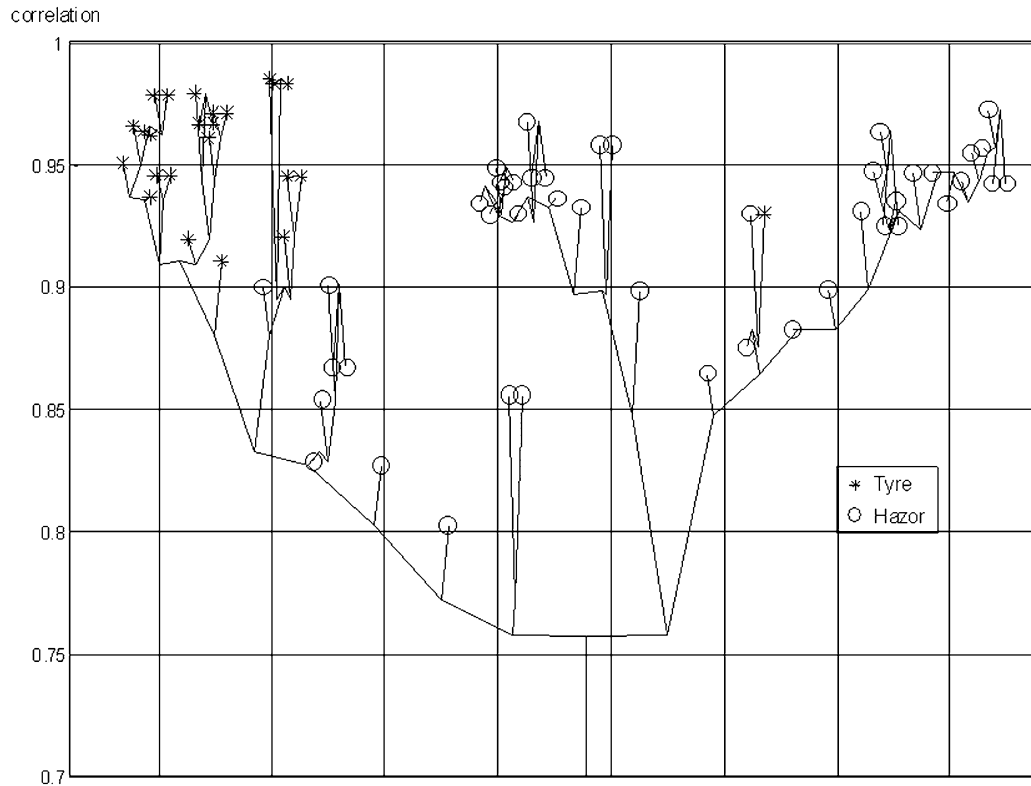


Fig. 8. The correlation tree of the combined assemblage of Hazor and Tyre jars.

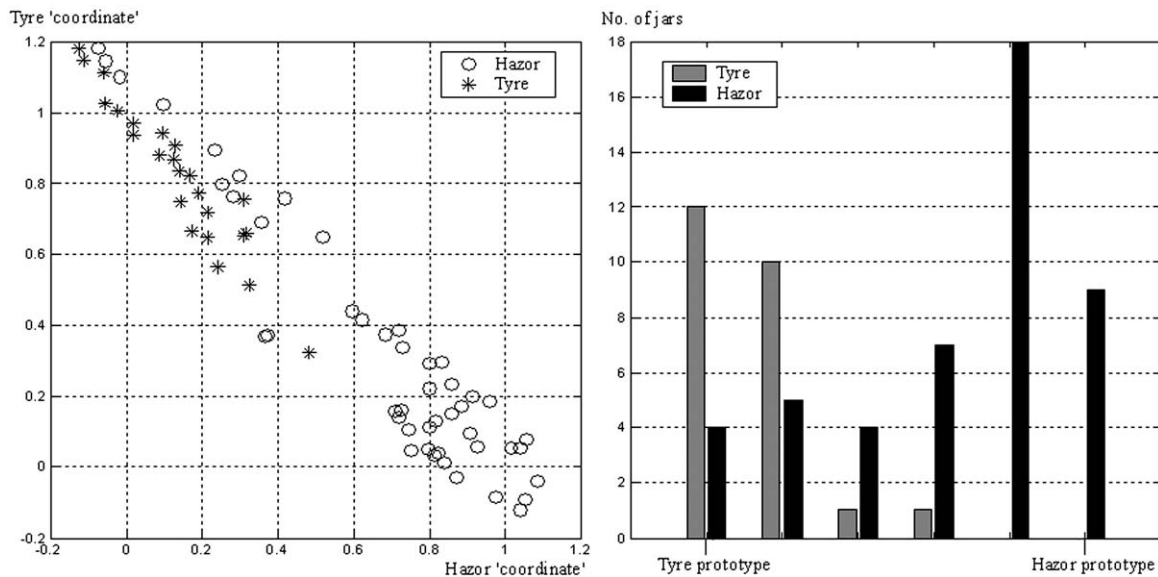


Fig. 9. The distribution of the whole assemblage in the prototypes plane (left) and along their axis (right).

assemblage with respect to these two prototypes, again using equation (12) and the results are presented in graphical form in (Fig. 9 [left]). Again, the distribution of the 'quality factors'  $\zeta_m$  is centered at the value  $\approx 0.3$  with a spread of  $\pm 0.15$  (FWHM—Full Width at Half

Maximum), supporting the use of only two prototypes in the analysis.

It is clear that most of the jars from Tyre demonstrate large correlations with the Tyre prototype, and their spread is rather low, indicating morphological uni-

formity. In contrast, the points representing jars from Hazor occupy a larger domain, showing, sometimes, larger affinity to the Tyre prototype than to the Hazor prototype. Thus even though the Hazor jars represent on average a specific type, it is not as uniform as the Tyre assemblage. Computing the distribution of the interpolating parameters  $\mu$  (equation (14)), provides a clear summary of the analysis (Fig. 9 [right]).

One may draw the following archaeological conclusions from this analysis: the lack of a significant morphological overlap raises doubts about the claims that the ‘torpedo’ jar assemblages indicate commercial links between Hazor and Tyre, as suggested by Geva [14]. The higher inner similarities observed in the assemblage of jars at Tyre supports the possibility that they were produced locally, as suggested by Bikai [5], possibly in a single workshop. There is still a possibility that *some* of the jars found at Hazor were actually made in Tyre, and perhaps even one or two of the ones found at Tyre were Hazorite—such hypotheses can now be tested by directed archaeometric tests on a very limited subset; but the ‘torpedo jar’ phenomenon *as a whole* does not indicate mass-trade in any one direction.

Thus, a different explanation is required to explicate on the one hand the *general* similarity between the jars at Hazor and Tyre and on the other—the wider spread of the Hazor jars as well as the few outliers in each group, but this is not our purpose here.

#### 4. Summary and future prospects

The two examples presented above show that the computerized typology and classification which we propose, meets with our original requirements. It provides an objective, sensitive and quantitative tool for typological studies of ceramics. The method is sufficiently general and versatile to accommodate a large variety of objects, sorting criteria or constraints. We are now applying it in various other problems of archaeological interest.

The main source of error in the present analysis is due to the fact that the information is derived from hand-drawn profiles, whose accuracy cannot be assessed. The intermediate step of scanning introduces further errors. Moreover, because of the high costs of draftsmanship and the printing of traditional reports, little of the excavated material is presented in full graphic form, and the choice of profiles available for analysis may reflect the bias and taste of the original authors. Using mechanical or electro-optical computerized drawing devices together with their accompanying software could appreciably reduce both sources of error. We are currently testing such systems.

Even if the computerized typology would only be able to provide an initial clustering of the archaeological

data, it will still offer the archaeologist a pre-selected set, thus reducing significantly the time needed for a meaningful detailed analysis. Our ultimate aim, however, is to optimize this process and turn it to an interactive, iterative analysis, with much higher resolution and reliability. Achieving this goal would certainly remove some of the most serious obstacles, which presently hamper morphological typologies and comparative studies.

Efficient and accurate recording and digitization of the artifacts; data-bases constructed to meet the specific requirements of storage and retrieval of such data; and efficient and versatile methods for shape analysis, alongside advanced sorting and clustering algorithms are prerequisites to constructing a tool which can replace the traditional ‘hunt for parallels’.

The method outlined above may on the one hand reveal hitherto unnoticed attributes and correlations, and on the other—investigate phenomena which could indeed be postulated, but not seriously investigated on the basis of traditional representations in site reports. A case in point are assessments of the mode of production of pottery, *inter alia* the question whether ceramic specialization and mass production (e.g., [8]) can be identified by typological analysis. Establishing, objectively, an exceptionally high degree of uniformity of particular attributes in a group of vessels could point to such phenomena.

Another example concerns the possibility to identify shared motor habit patterns of the producers of the pots. This may involve mechanisms resulting from manual proficiency, hand-eye coordination, subconscious habitual physiologically based postures and movements, that recur while the pots are thrown. These protocols manifest themselves in those (often more covert) attributes that archaeologists employ to characterize the pots they study. The effect of these patterns, or skills, on pottery production is well documented ethnographically (e.g., [3, p. 206]), but rarely has this issue been investigated regarding the archaeological record (cf. also [7 esp. p. 198 and references therein; 20, 21]). Given that some shape attributes, like the overall shape of the vessels, and their size, are due to conscious mental templates (‘traditions’) and/or functional/symbolic considerations, how similar and in what respect should two vessels be, in order to further assume shared motor habits between their producers? The ability to assess with high-resolution parameters of morphological variation/uniformity is a pre-requisite in this, and any other study concerning intra- and inter-assemblage diversity.

#### Acknowledgements

This research is supported by a BIKURA grant from the Israel Science Foundation, and by the Kimmel



Center for Archaeological Sciences in the Weizmann Institute of Science.

## References

- [1] K. Adler, M. Kampel, R. Kastler, M. Penz, R. Sablatnig, K. Schindler, S. Tosovic, Computer aided classification of ceramics—achievements and problems, in: *Proc. of 6th Intl. Workshop on Archaeology and Computers*, Vienna, Austria, 2001.
- [2] W.P. Anderson, Sarepta I: The late Bronze Age and Iron Age strata of area II, Y. Publications de l'université Libanaise, Section des études archéologiques II. Beyrouth, Université Libanaise, 1988.
- [3] D.E. Arnold, *Ceramic Theory and Cultural Process*, University Press, Cambridge, 1989.
- [4] M.E. Aubet, *The Phoenicians and the West*, University Press, Cambridge, 2000.
- [5] P.M. Bikai, Observations on archaeological evidence for the trade between Israel and Tyre, *Bulletin of the American Schools of Oriental Research* 258 (1985) 71–72.
- [6] P.M. Bikai, *The Pottery of Tyre*, Aris & Philips, Warminster, 1978.
- [7] C. Carr, A unified middle-range theory of artifact design, in: C. Carr, J.E. Neitzel (Eds.), *Style, Society and Person: Archaeological and Ethnological Perspectives*, Plenum Press, New York and London, 1995.
- [8] C.L. Costin, Craft specialization: issues in defining, documenting, and explaining the organization of production, in: M.B. Schiffer (Ed.), *Archaeological Method and Theory* 3, The University of Arizona Press, Tucson, 1991, pp. 1–56.
- [9] P.D. Curtin, *Cross-cultural Trade in World History*, University Press, Cambridge, 1984.
- [10] P. Durham, P. Lewis, S. Shennan, Artefact matching and retrieval using the Generalised Hough Transform, in: J. Wilcock, K. Lockyear (Eds.), *Computer Applications and Quantitative Methods in Archaeology* 1993, BAR Int. Ser. 598, 1995, pp. 25–30.
- [11] D.P. Fairney, P.T. Fairney, On the accuracy of point curvature estimators in a discrete environment, *Image and Vision Comp* 12 (1994) 259–265.
- [12] P. Garnsey, K. Hopkins, C.R. Whittaker, *Trade in the Ancient Economy*, University of California Press, Berkeley, 1983.
- [13] J. Gero, J. Mazzullo, Analysis of artifact shape using Fourier series in closed form, *Journal of Field Archaeology* 11 (3) (1984) 315–322.
- [14] S. Geva, Archaeological evidence for the trade between Israel and Tyre, *Bulletin of the American Schools of Oriental Research* 248 (1982) 69–72.
- [15] A. Gilboa, *Southern Phoenicia During Iron Age I-IIa in the Light of the Tel Dor Excavations*, The Institute of Archaeology, The Hebrew University, Jerusalem, 2001.
- [16] A. Gilboa, The typology of Iron Age pottery and the chronology of Iron Age assemblages, in: E. Stern, et al., *Excavations at Tel Dor, final report volume IB: areas A and C. Qedem Reports 2*, The Institute of Archaeology: The Hebrew University, Jerusalem, 1995.
- [17] A. Gilboa, I. Sharon, An archaeological contribution to the early Iron Age chronological debate: Alternative chronologies for Phoenicia and their effects on the Levant, Cyprus and Greece, *Bulletin of the American Schools of Oriental Research* (in press).
- [18] A. Gilboa, I. Sharon, Early Iron Age radiometric dates from Tel Dor: preliminary implications for Phoenicia, and beyond, *Radiocarbon* 43 (3) (2001) 1343–1351.
- [19] M.B. Hagstrum, J.A. Hildebrand, The 'two-curvature' method for reconstructing ceramic morphology, *American Antiquity* 55 (2) (1990) 388–403.
- [20] J.N. Hill, Individual variability in ceramics and the study of prehistoric social organization, in: J.N. Hill, J. Gunn (Eds.), *The Individual in Prehistory: Studies in Variability in Style in Prehistoric Technologies*, Academic Press, New York, 1977, pp. 55–108.
- [21] J.N. Hill, Individuals and their artifacts: an experimental study in archaeology, *American Antiquity* 43 (1978) 245–257.
- [22] J.N. Hill, R.K. Evans, A model for classification and typology, in: D.T. Clarke (Ed.), *Models in Archaeology*, Methuen and Company, London, 1972, pp. 231–273.
- [23] <<http://www.prip.tuwien.ac.at/Research/ArcheologicalSherds/>>
- [24] <<http://3dk.asu.edu/>>
- [25] <<http://student.ulb.ac.be/~claugero/PhD/potteries/index.html>>
- [26] <<http://researchweb.watson.ibm.com/peru/>>
- [27] <<http://www.dcc.unicamp.br/~stolfi/EXPORT/projects/fragments/>>
- [28] <<http://www.lems.brown.edu/vision/extra/SHAPE/>>
- [29] A.D. Kalvin, A. Remy, L.J. Castillo, K. Morla, E. Nolasco, J. Prado, V. Fernandez, R. Franco, G. Wiese, Computer-aided reconstruction of a pre-Inca temple ceiling in Peru, *Computer Applications in Archaeology (CAA 97)*, University of Birmingham, UK, 1997.
- [30] C.K. Lee, R.M. Haralick, K. Deguchi, Estimation of curvature from sampled noisy data, in: *Int. Conference on Computers Vision and Pattern Recognition CVPR (93)*, New York, 1993, pp. 536–541.
- [31] M.N. Leese, P.L. Main, An approach to the assessment of artefact dimension as descriptors of shape, in: J.G.B. Haigh (Ed.), *Computer Applications in Archaeology 1983*, University of Bradford, School of Archaeological Sciences, Bradford, 1983, pp. 171–180.
- [32] H.C.G. Leitao, J. Stolfi, A multi-scale method for the re-assembly of fragmented objects, *British Machine Vision Conference—BMVC 2000* 2, 2000, pp. 705–714.
- [33] P.H. Lewis, K.J. Goodson, Images, databases and edge detection for archaeological object drawings, in: K. Lockyear, S. Rahtz (Eds.), *Computer Applications and Quantitative Methods in Archaeology* 1990, 1991, pp. 149–153.
- [34] F. Leymarie, D. Cooper, M.S. Joukowsky, B. Kimia, D. Laidlaw, D. Mumford, E. Vote, *The SHAPE Lab.—new technology and software for archaeologists, Computing Archaeology for Understanding the Past (CAA 2000)*, Archaeopress, Oxford, UK, 2001, pp. 79–89.
- [35] F. Leymarie, M.D. Levine, Curvature morphology, *Computer Vision and Robotics Laboratory*, McGill University, Montreal, Quebec, Canada, 1988.
- [36] G. Liming, L. Hongjie, J. Wilcock, The analysis of ancient Chinese pottery and porcelain shapes: a study of classical profiles from the Yangshao culture to the Qing dynasty using computerized profile data reduction, cluster analysis and fuzzy boundary discrimination, *Computer Applications and Quantitative Methods in Archaeology* 1989, 1989, pp. 363–374.
- [37] F. Mokhtarian, M. Bober, *Curvature Scale Space Representation, and MPEG-7 Standardization* 25, Kluwer Academic Publishers, Dordrecht, The Netherlands, 2003.
- [38] C. Orton, *Mathematics in Archaeology*, University Press, Cambridge, 1980.
- [39] C. Orton, P. Tyres, A. Vince, *Pottery in Archaeology*, University Press, Cambridge, 1993.
- [40] J. Pobelome, J. van den Brandt, B. Michiels, G. Evesever, R. Degeest, M. Walkens, Manual drawing versus automated recording of ceramic, in: M. Walkens (Ed.), *Sagalasos IV Acta Archaeologica Lovaniensia Monographiae* 9, Leuven, 1997, pp. 533–538.

- [41] H. Pottmann, M. Peternell, B. Ravani, An introduction to line geometry with applications, *Computer Aided Design* 31 (1999) 3–16.
- [42] A. Razdan, D. Liu, M. Bae, M. Zhu, G. Farin, Using geometric modeling for archiving and searching 3D archaeological vessel, in: *International Conference on Imaging Science, Systems, and Technology CISST 2001*, Las Vegas, 2001.
- [43] R. Sablatnig, C. Menard, Computer based acquisition of archaeological finds: the first step towards automatic classification, in: P. Moscati, S. Mariotti (Eds.), *The 3rd International Symposium on Computing and Archaeology*, Vol. 1, Rome, 1996, pp. 429–446.
- [44] J. Sabloff, C.C. Lamberg-Karlovsky (Eds.), *Ancient Civilization and Trade*, University of New Mexico Press, Albuquerque, 1975.
- [45] I. Sharon, A. Gilboa, The SKL Town: Dor in the Early Iron Age, in: M. Artzy, A.E. Killebrew, G. Lehmann (Eds.), *Philistines and Other Sea People*, Brill, Leiden, in press.
- [46] R. Whallon, J.A. Brown (Eds.), *Essays on Archaeological Typology*, Center for American Archaeology Press, 1982.
- [47] Y. Yadin, Y. Aharoni, R. Amiran, T. Dothan, M. Dothan, I. Dunayevsky, J. Perrot, *Hazor III–IV: An Account of the Third and Fourth Seasons of Excavation, 1957–1958*, The Hebrew University, Jerusalem, 1961.
- [48] Y. Yadin, Y. Aharoni, R. Amiran, T. Dothan, I. Dunayevsky, J. Perrot, *Hazor II: An Account of the Second Season of Excavation, 1956*, The Hebrew University, Jerusalem, 1960.